16TH EUROPEAN CONFERENCE ON EARTHQUAKE ENGINEERING THESSALONIKI 18 - 21 JUNE 2018

SCENARIO-BASED SEISMIC RISK ASSESSMENT FOR MALAWI USING IMPROVED INFORMATION ON EARTHQUAKE SOURCES AND LOCAL BUILDING CHARACTERISTICS

Katsuichiro GODA[1], Panos KLOUKINAS[2], Raffaele DE RISI[3], Michael HODGE[4], Innocent KAFODYA[5], Ignasio NGOMA[6], Juliet BIGGS[7], Adam CREWE[8], Ake FAGERENG[9], John MACDONALD[10]

ABSTRACT

This study presents scenario-based seismic hazard and risk assessments for Malawi using improved information on earthquake sources and local building characteristics. A case study is focused upon areas near the Bilila-Mtakataka Fault (south of Lake Malawi). The Bilila-Mtakataka Fault is approximately 130-km long, and six segments can be identified along the scarp, which might rupture individually or altogether. The earthquake source models take into account different rupture scenarios in terms of fault geometry and earthquake magnitude. To represent current building stock in the target region, building surveys are conducted to develop a realistic seismic risk model. Moreover, seismic fragility models for typical masonry buildings in Malawi are developed based on pushover analysis of finite-element models. Finally, all improved model components are integrated to carry out the seismic hazard and risk assessments in Central-Southern Malawi. The new seismic hazard and risk assessments will inform the baseline seismic risk more accurately.

Keywords: Malawi; Seismic hazard and risk; Earthquake fault; Building survey; Masonry buildings

1. INTRODUCTION

Enhancing disaster preparedness and resilience is one of the key global challenges for sustainable development. The UNISDR's Sendai Framework sets out a road map for reducing natural disaster risks in developing countries (http://www.unisdr.org/we/coordinate/sendai-framework). The essential steps to achieve this goal are to quantify the risk to society (e.g. population and built environment), which is comprised of three elements, i.e. hazard, exposure, and vulnerability, and then to develop suitable disaster risk reduction strategies considering socioeconomic conditions of the countries and involved stakeholders/communities.

Malawi is a landlocked country in Sub-Saharan Africa and is one of the least developed countries around the world. In Malawi, seismic risk is not negligible for three reasons. Firstly, Malawi is located within the western branch of the East African Rift System, where large earthquakes of M_w7+ occurred in the past (e.g. 1910 Rukwa earthquake in Tanzania, Poggi et al. 2017). In the last few decades,

[1]Reader, University of Bristol, Bristol, United Kingdom, katsu.goda@bristol.ac.uk
[2]Senior Research Associate, University of Bristol, Bristol, United Kingdom, p.kloukinas@bristol.ac.uk
[3]Research Associate, University of Bristol, Bristol, United Kingdom, raffaele.derisi@bristol.ac.uk
[4]PhD Candidate, University of Bristol, Bristol, United Kingdom, HodgeMS@cardiff.ac.uk
[5]Lecturer, University of Malawi Polytechnic, Blantyre, Malawi, ikafodya@poly.ac.mw
[6]Associate Professor, University of Malawi Polytechnic, Blantyre, Malawi, ingoma@poly.ac.mw
[7]Reader, University of Bristol, Bristol, United Kingdom, juliet.biggs@bristol.ac.uk
[8]Reader, University of Bristol, Bristol, United Kingdom, a.j.crewe@bristol.ac.uk
[9]Reader, Cardiff University, Cardiff, United Kingdom, FagerengA@cardiff.ac.uk
[10]Reader, University of Bristol, Bristol, United Kingdom, john.macdonald@bristol.ac.uk

Malawi experienced several moderate (M_w6+) events, such as the 1989 Salima earthquake (Gupta and Malomo 1995) and the 2009 Karonga earthquake (Biggs et al. 2010), which caused significant damage and loss. Secondly, traditional masonry structures are unreinforced and seismically vulnerable (World Housing Encyclopedia 2002), and currently adequate seismic design provisions and construction practice are not in place. Thirdly, Malawi has been experiencing rapid population growth (annual growth rate of about 3%), and more people migrate into informal settlements surrounding major cities, such as Lilongwe and Blantyre (UN-Habitat 2010).

The first step towards achieving improved seismic resilience in Malawi is to assess earthquake hazard and risk accurately. However, due to lack of basic information, such as geological and geomorphological data, seismicity data, building data, and strength data of construction materials, seismic hazard and risk assessments involve major uncertainties. To apply risk management decisions in Malawi, integrated tools for assessing seismic risk are essential, but they are not available in the public domain. Hodge et al. (2015) and Goda et al. (2016) attempted to address these important problems by developing the first-generation probabilistic seismic hazard and risk models for Malawi based on fault-based earthquake source models and global building-collapse prediction models. The results provided useful insight regarding the impact of hazard-exposure-vulnerability characteristics on the seismic risk in Malawi. The current seismic hazard and risk models for Malawi need to be improved by: (i) incorporating detailed fault mapping and earthquake rupture potential, (ii) implementing new ground motion prediction models, (iii) considering more realistic typology of local building stock, and (iv) implementing seismic fragility models that are developed based on structural characteristics of local/regional buildings in Malawi. It is important to point out that all these improvements make the developed tools more comprehensive and enhance seismic risk mitigation actions.

This study presents scenario-based seismic hazard and risk assessments for Malawi using improved information on earthquake sources and local building characteristics. The scenario-based shake maps and earthquake impact estimation tools are particularly useful for earthquake risk management purposes (e.g. Wald et al. 2005, Earle et al. 2009). A case study is focused upon several cities and townships near the Bilila-Mtakataka Fault (BMF, Jackson and Blenkinsop 1997) in Central-Southern Malawi, such as Salima, Golomoti, Balaka, and Liwonde. The BMF is approximately 130-km long, and may consist of six segments along the scarp (Hodge et al. 2017). Therefore, the earthquake source model should take into account various rupture scenarios in terms of fault geometry and earthquake magnitude. From a ground motion modeling perspective, newer prediction equations, such as the NGA-West2 (e.g. Boore et al. 2014), can be adopted. To represent current building stock in the target region, building surveys are conducted to develop a realistic seismic risk exposure model. The local building information of Malawian settlements is integrated with the 2008 national census data (National Statistical Office of Malawi 2008) and up-to-date population data, such as World Population Review (http://worldpopulationreview.com/countries/malawi-population/). Based on the survey results, finite-element models for typical masonry buildings in Central-Southern Malawi are developed and are used to develop seismic fragility models for the masonry wall structures. Finally, all improved model components are integrated to carry out the updated seismic risk assessments for the selected locations near the BMF. The updated seismic hazard and risk assessments will inform the baseline regional seismic risk more accurately.

2. METHODOLOGY

2.1 Seismic Hazard and Risk Analysis

A general risk assessment framework, i.e. *risk* = *hazard* × *exposure* × *vulnerability*, can be adopted to perform scenario-based earthquake hazard and risk analyses for Malawi. The approach implemented in this study is probabilistic and captures the uncertainties associated with key elements of the analyses. The analysis methodology is illustrated in Figure 1.

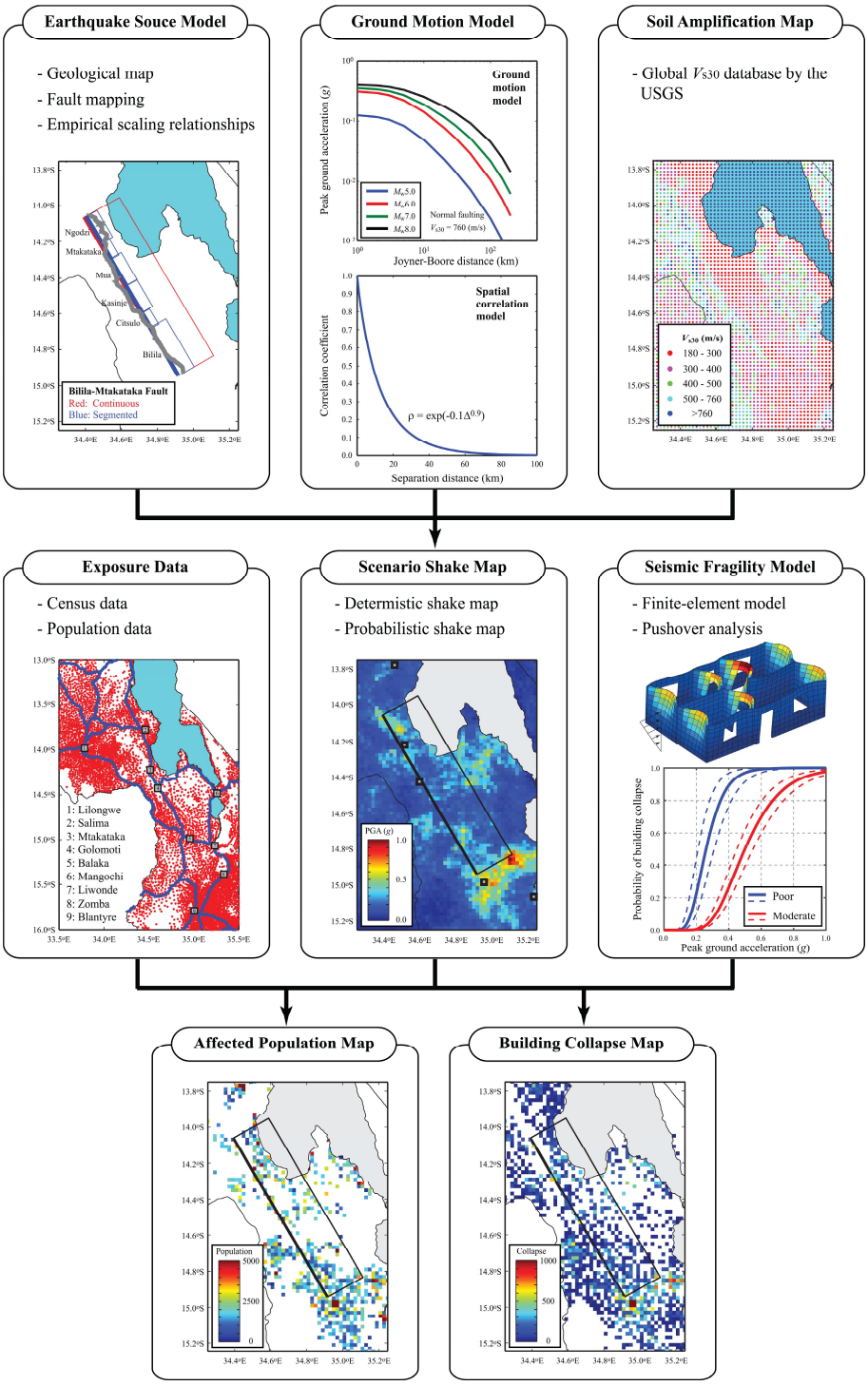

Figure 1. Scenario-based seismic hazard and risk assessment framework for Malawi

The seismic hazard module consists of earthquake source modeling and ground motion modeling, supplemented by the near-surface shear-wave velocity information (see the top row of Figure 1). The earthquake source model is developed based on available geological and geomorphological information, which essentially determines the geometry of potential earthquake rupture planes. Given the fault geometry and potential large seismogenic thickness of the upper crust (Jackson and Blenkinsop 1993), earthquake source scaling relationships are applied to estimate other earthquake source parameters, such as earthquake slip and magnitude. The earthquake source model is then used to simulate the spatial distribution of ground shaking in terms of adopted seismic hazard parameters of interest, such as peak ground acceleration (PGA). In simulating ground motion intensities at multiple

sites, a ground motion model is applied together with a spatial correlation model and local site information to generate realistic ground motion fields. The above set-up facilitates the generation of probabilistic scenario shake maps in the region of interest (see the central panel in Figure 1).

Subsequently, the regional earthquake impact is evaluated by integrating probabilistic shake maps with population information obtained from the census data and with seismic fragility models of building archetype/topology (see the left and right panels in the middle row of Figure 1). The seismic fragility model can be developed by utilizing the existing information on building stock, by conducting local building surveys, and by performing suitable structural modeling and analyses. These will lead to the generation of probabilistic earthquake risk maps in terms of affected population experiencing certain levels of ground shaking and in terms of building collapse, and will provide valuable insight for earthquake risk management.

2.2 Model Components

This section provides more details of the key model components of the seismic hazard and risk assessment methodology by focusing upon the BMF in Central-Southern Malawi.

2.2.1 Earthquake rupture scenarios for the Bilila-Mtakataka Fault

The Bilila-Mtakataka Fault extends from 20 km north of Mtakataka southward to around 5 km north of Balaka. Its scarp length is about 130 km and is shown in Figure 2 (Hodge et al. 2017). The scarp runs sub-parallel with Motorway No 5, and its height ranges between 5 m and 20 m, with an average of 11 m. In places, the scarp can be easily recognized along Motorway No 5 but begins to step back in a series of zig-zag patterns north of Mtakataka. Hodge et al. (2017) studied satellite imagery and conducted geological field mapping of the BMF, and identified six segments along its length, i.e. Ngodzi, Mtakataka, Mua, Kasinje, Citsulo, and Bilila segments from North to South (see Figure 2). They hypothesized that the earthquake rupture of the BMF could occur along the entire length, discrete as segments or multiple segments, and produced two types of rupture models (i.e. continuous and segmented cases). They also suggested that the reduced scarp height at the Citsulo segment may suggest a break in fault continuity between the northern segments and the southern Bilila segment, indicating potential evidence for single segment ruptures along Bilila. These earthquake rupture models are also shown in Figure 2. The geometrical information of the BMF rupture models is summarized in Table 1. The expected faulting mechanism for the BMF is normal faulting.

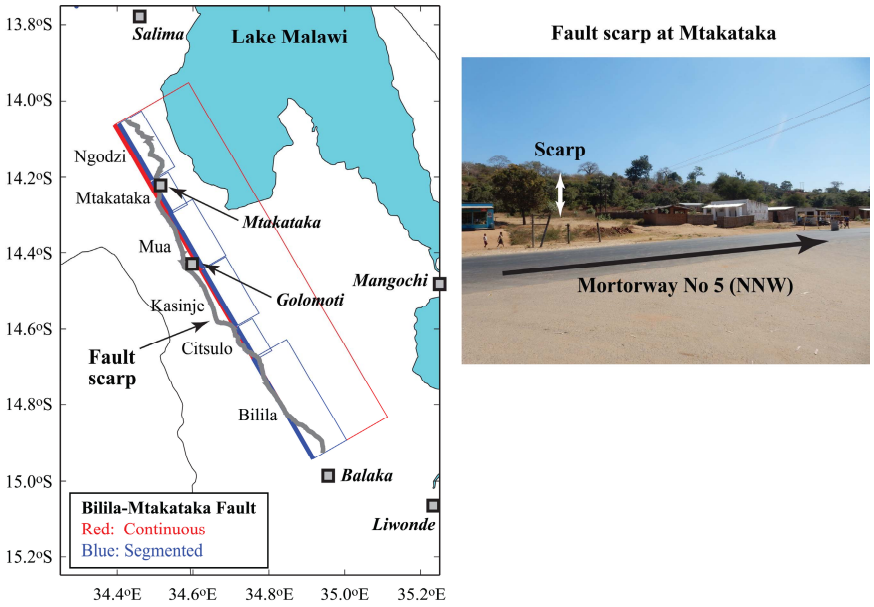

Figure 2. Locations of the Bilila-Mtakataka Fault scarp and nearby settlements

Table 1. Geometry of the Bilila-Mtakataka Fault (Hodge et al. 2017)

Rupture case	Scarp length (km)	Fault length (km)	Strike (º)	Upper-left corner		Width[1] (km)	Slip (m)	M_w
				Lat. (º)	Lon. (º)			
Continuous	128	113	330	-14.9427	34.9168	48.6	2.67	7.8
Ngodzi segment	21	19	330	-14.2071	34.4921	14.6	0.20	6.2
Mtakataka segment	13	11	330	-14.2965	34.5437	10.6	0.10	5.7
Mua segment	21	19	330	-14.4408	34.6271	14.6	0.20	6.2
Kasinje segment	22	19	330	-14.5921	34.7144	15.0	0.22	6.2
Citsulo segment	13	11	330	-14.6815	34.7660	10.6	0.10	5.7
Bilila segment	38	34	330	-14.9427	34.9168	21.6	0.47	6.7

[1] The dip angle is assumed to be 60º.

To fully define the fault geometry and magnitude of the earthquake rupture based on the scarp/fault length, the fault geometry and magnitude are estimated based on empirical source scaling laws. For the estimation, self-similar scaling laws that relate the fault length L, fault width W, and average slip D to moment magnitude, which has been recently developed by Thingbaijam et al. (2017) based on an extensive set of finite-fault source models, are adopted. The scaling relationships that are applicable to normal-faulting events having M_w5.9 to M_w8.4 are given by (Thingbaijam et al. 2017):

$$\log_{10}(L) = 0.485 \times M_w - 1.722 + 0.128 \times \varepsilon \quad (1)$$

$$\log_{10}(W) = 0.323 \times M_w - 0.829 + 0.128 \times \varepsilon \quad (2)$$

$$\log_{10}(D) = 0.693 \times M_w - 4.967 + 0.195 \times \varepsilon \quad (3)$$

where ε is the standard normal variable with zero mean and unit standard deviation. Using Equations 1 to 3, values of the fault width, average slip, and moment magnitude can be determined for a given value of L. The results are indicated in Table 1. Because the above scaling relationships are obtained by ensuring the self-similarity, the order of estimations of the earthquake parameters does not affect the results.

2.2.2 Ground motion simulations

Empirical ground motion models can be used to synthesize realistic ground motion fields for a given earthquake scenario. A suitable ground motion prediction model together with a spatial correlation model of intra-event variability needs to be selected (Goda and Hong 2008). In this study, due to the lack of regional strong ground motion data and region-specific ground motion models for the East African Rift System (Hodge et al. 2015, Poggi et al. 2017), a global ground motion model for shallow crustal earthquakes by Boore et al. (2014) is adopted. Median ground motions for four earthquake magnitudes as a function of distance are illustrated in Figure 3a. For the spatial correlation model of intra-event variability, the spatial correlation model that is illustrated in Figure 3b is adopted based on the previous studies (Goda and Hong 2008).

By combining the ground motion model by Boore et al. (2014) and the spatial correlation model, multiple realizations of spatially correlated ground motion fields can be generated at multiple sites (i.e. probabilistic shake maps). The consideration of a realistic spatial correlation model for intra-event variability of the ground motion model is important, especially when evaluating regional earthquake impact, in terms of total affected population or number of collapsed buildings. In contrast, deterministic shake maps can be obtained by ignoring the variability of the ground motion model.

In implementing a ground motion model for shake map generation, the earthquake scenario is usually characterized by a set of earthquake source parameters, such as earthquake magnitude, faulting type, and fault location/geometry, whereas additional parameters, such as source-to-site distances and local

ground conditions, need to be specified for individual locations. For the BMF, earthquake scenarios can be defined by referring to the seven rupture cases (i.e. continuous case and six segmented cases), as indicated in Figure 2 and Table 1. For gridded locations in Central-Southern Malawi with interval of 0.02º (approximately, 2.2 km), source-to-site distances can be computed. For the local site conditions at the grid locations, estimated values of average shear-wave velocity in the uppermost 30 m V_{s30} at the grid locations are obtained from the USGS's V_{s30} database (Wald and Allen 2007).

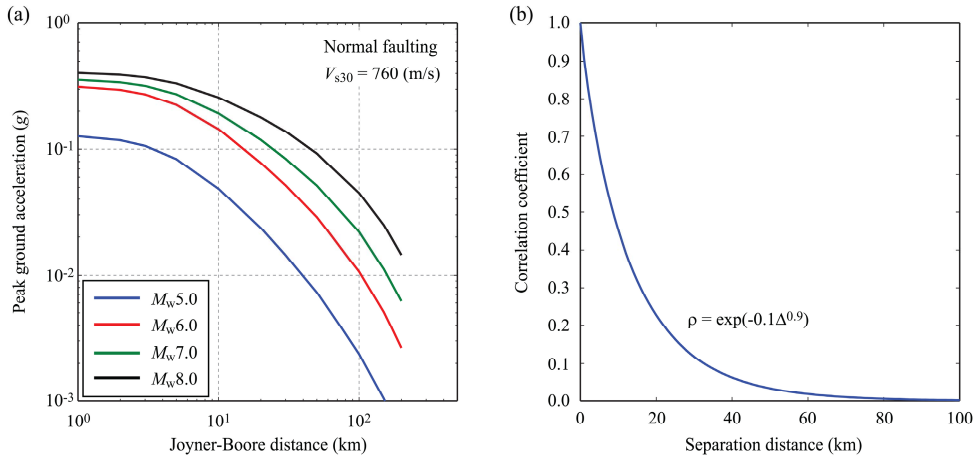

Figure 3. (a) Predicted peak ground accelerations at a reference site condition of V_{s30} = 760 m/s for different earthquake scenarios, and (b) spatial correlation model used for ground motion simulations

2.2.3 Population and building characteristics in Central-Southern Malawi

The population in Malawi has been in rapid increase with annual growth rate of about 3%, with the current estimate of the population of about 18.6 million. The corresponding number of households are ~4.2 million, assuming 4.4 persons per household (National Statistical Office of Malawi 2008). The majority of its population is rural and agricultural. Notably, the urban population is also increasing rapidly, which was 14.6% in the 2008 census. This number is expected to increase to ~30% by 2025 and to ~50% by 2050 (UN-Habitat 2010).

Because of high price of houses offered by the formal construction sector in Malawi and inaccessibility of affordable housing loans, the majority of housing supply is met by the informal construction sector. This in turn leads to ordinary houses being constructed with low-quality, locally-made clay bricks assembled together into generally unsupervised, poorly-designed masonry structure layouts (Ngoma 2005, UN-Habitat 2010). Consequently, seismic vulnerability of the housing stock in Malawi is high (World Housing Encyclopedia 2002).

In the 2008 census, dwelling is categorized into three types: traditional (made of rammed earth, daub and wattle, or timber walls and lightweight thatched roof), semi-permanent (made of unburnt clay bricks and thatched roof), and permanent (made of burnt clay brick and iron sheet roof). Approximately, proportions of traditional, semi-permanent, and permeant dwelling were 28%, 44%, and 28%, respectively. It is noted that the building stock characteristics in Malawi are changing rapidly, replacing traditional/semi-permanent houses with more permanent ones (UN-Habitat 2010).

To understand the regional characteristics of current building stock, building surveys were conducted in 2016 and 2017 by focusing upon cities and towns near the BMF (Figure 2). The selected locations were secondary-urban district centers and small townships. The covered areas of the surveys were limited due to the available resources, and the results are not intended for generating a complete and comprehensive building stock database for Central-Southern Malawi. Rather, they should be used as supplementary information to modify the census data in light of current rapid demographic changes in Malawi. To relate the survey results to the 2008 census data, several census enumeration areas (EA) were selected as representative sub-areas by inspecting population/household numbers and Google

images (Figure 4). In each EA, two types of building surveys, i.e. quick walk-through surveys and detailed surveys of individual buildings, were performed to collect data; the gathered data can be extrapolated to estimate the building stock information in wider areas and to produce numerical models of buildings for seismic vulnerability assessment (Section 2.2.4).

The quick walk-through surveys were conducted using GPS geo-tagging devices in eight EAs in Salima, Mtakataka, Golomoti, Balaka, and Mangochi. Based on observed similarity of building typologies, the surveyed locations can be grouped into: (i) secondary-urban areas developed by the formal construction sector (Salima), (ii) secondary-urban areas developed by the informal construction sector (Salima, Mangochi, and Balaka), and (iii) rural township areas (Golomoti and Mtakataka). During the surveys, buildings were classified in terms of their basic structural characteristics: wall material (burnt/unburnt bricks), wall thickness (single-skin and double-skin walls), presence of lintels above openings and their types (wooden, concrete, concrete ring beam), shape of layout (regular/irregular), and roofing shape (mono-pitched, gable, and hipped). The survey results in terms of the household number are consistent with the 2008 census data. A summary of the building surveys, in comparison with the 2008 census data, is shown in the lower-left panel of Figure 4. The results indicate that the proportions of the permanent buildings (i.e. fired brick masonry) in the surveyed areas are significantly greater than those indicated in the census data. In addition, single-skin walls are more common in rural areas than secondary-urban areas.

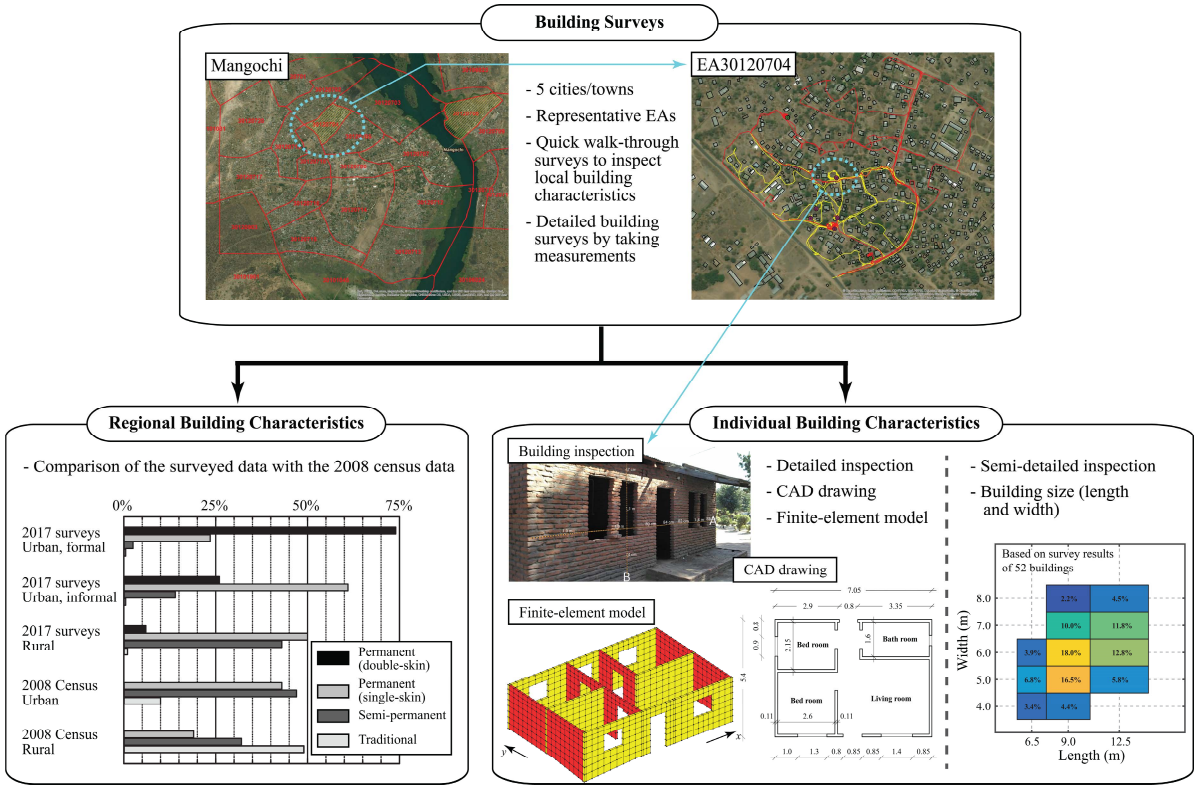

Figure 4. Building surveys and characteristics of masonry houses in Central-Southern Malawi

For structural modeling, more detailed information, such as dimension and material type (e.g. brick and mortar) of a building, is necessary. A notable observation of brick construction in Malawi is significant variation of brick and mortar; the size of bricks varies significantly, and material properties of brick and mortar are generally poor and can be very different depending on locations because of local availability of materials. These variations essentially result in different seismic performance and failure modes of the structural components subjected to loading. In addition to the material properties, the strength of a masonry wall element is highly affected by geometrical factors, such as the type of brick bonding, thickness of the joints, openings, and support conditions.

To collect more specific information of typical buildings in Central-Southern Malawi, a few buildings within each EA district were selected for detailed inspections, and measurements of geometry and layout were taken using laser/tape measures and Google Tango devices (i.e. quick photographic surveys). During the surveys, detailed measurements of 16 buildings were taken by inspecting both outside and inside of the buildings, whereas semi-detailed inspections of 52 buildings were conducted to measure building dimensions by selecting houses per every 5 buildings that were visited by the survey teams. These facilitate the semi-automated construction of CAD models of the surveyed buildings. Examples of the detailed and semi-detailed surveys of individual buildings are presented in the lower-right panel of Figure 4. By analyzing all gathered data, a typical house size can be specified as a layout having the width of about 6 m and the length of about 9 m.

2.2.4 Seismic vulnerability of masonry buildings in Central-Southern Malawi

Numerous studies have been conducted to assess seismic vulnerability of masonry structures. Approaches that have been implemented vary significantly from damage observations, experiments, numerical modeling, to combinations of these. Among applicable numerical approaches, simpler methods are to carry out the limit analysis (e.g. Milani et al. 2007) and equivalent-frame analysis (e.g. Quagliarini et al. 2016). Alternatively, more computationally-extensive methods, such as macro-element modeling (e.g. Lagomarsino et al. 2013), finite-element modeling with distributed plasticity (e.g. Raka et al. 2015), and discrete-element modeling (e.g. Caliò et al. 2012), can be implemented.

In this study, the equivalent continuum approach (i.e. finite-element modeling) is adopted since this method only requires the definition of macroscopic mechanical properties (e.g. shear strength and friction coefficient). To make the developed numerical models and tools accessible to research/professional communities in Malawi, proprietary finite-element codes are not suitable for economic reasons. Therefore, an open-source free finite-element software OpenSees (McKenna 2011) is selected. In modeling a masonry building using OpenSees, the eight-node hexahedral brick element *SSPbrick* is used. Such modeling requires the definition of a multi-dimensional material model that is suitable for masonry structure. For this purpose, the Drucker-Prager material model (Drucker and Prager 1952), which is already implemented in OpenSees and is applicable to characterizing the masonry behavior, is considered. The parameters that are necessary to define the material can be related to the pure shear strength (cohesion) and the friction angle. To evaluate the structural behavior of the modeled masonry building under significant horizontal load, static nonlinear (pushover) analysis is carried out along the two main structural axes using an inverse triangular force distribution (Figure 5a). During the pushover analysis, all top points of the structure, which deflect in both in-plane and out-of-plane directions, are monitored, and mean displacement of the monitored points is considered to define the overall horizontal response of the structure (i.e. pushover curve).

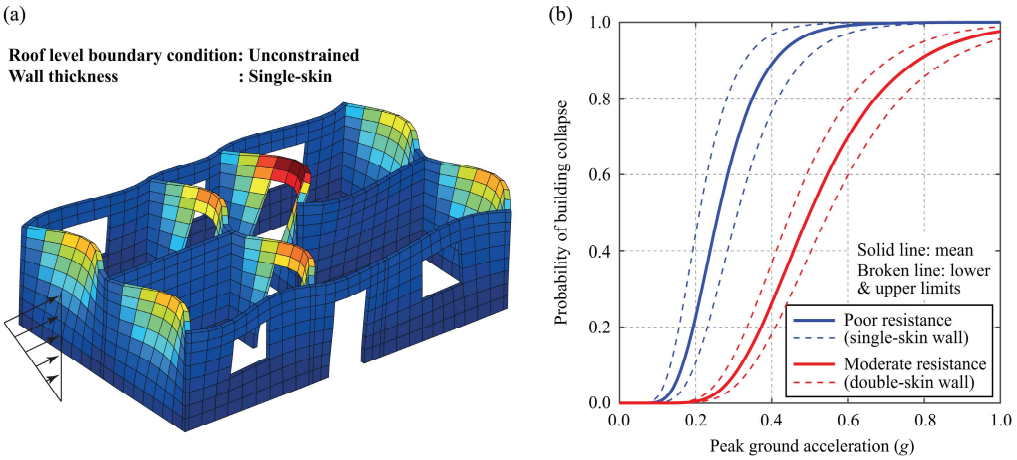

Figure 5. (a) Pushover analysis of a finite-element model for typical masonry house in Central-Southern Malawi, and (b) seismic fragility curves for two different masonry wall configurations

Subsequently, the obtained pushover curve is converted to a multi-linearized capacity curve corresponding to an equivalent single-degree-of-freedom system, and is then transformed to an incremental dynamic analysis (IDA) curve using the SPO2IDA tool (De Luca et al. 2013). The spectral acceleration corresponding to the flat part of the IDA curve is considered as the collapse capacity of the structure. The above-mentioned procedure produces a pushover curve for a given set of structural model parameters (e.g. Young's modulus, self-weight, shear strength, and compressive strength). To account for uncertainties of the structural parameters, these parameters are considered as random and 50 simulations are carried out. Finally, using the 50 pushover results, robust seismic fragility curves are developed, and are used for assessing the collapse risk of buildings in the form of seismic fragility function. Because the wall thickness (single-skin versus double-skin walls having thickness of 0.11 m and 0.23 m, respectively) has been identified as one of the critical parameters in determining the seismic vulnerability of masonry buildings, two sets of seismic fragility models for structural collapse are developed (i.e. '*poor*' and '*moderate*'); the mean, lower-, and upper-limit fragility curves for typical masonry buildings in Central-Southern Malawi are shown in Figure 5b.

3. RESULTS

3.1 Scenario-based Seismic Hazard and Risk Maps

In this section, probabilistic seismic hazard and risk maps are generated to demonstrate the potential regional impact due to two earthquake scenarios: (i) continuous rupture of the BMF along its entire length (M_w7.8) and (ii) rupture of a single geometrically defined segment, using the Bilila segment as an example (M_w6.7) (see Figure 2 and Table 1). In the ground motion simulations, uncertainties of PGA are characterized by a ground motion model and spatial correlation model (Figure 3). A realization of probabilistic PGA shake maps is shown for the continuous and Bilila rupture cases in Figure 6a and Figure 6d, respectively. The probabilistic shake maps exhibit heterogeneous distribution of PGA values within the rupture zone due to spatially correlated variability of the ground motion model with locally concentrated shaking intensities. The comparison of the two maps highlights the effects of the earthquake size, resulting in very different spatial areas of strong ground motions.

Next, scenario maps of the distribution of population experiencing PGA > 0.2 *g* for the continuous and Bilila rupture cases are produced and presented in Figure 6b and Figure 6e, respectively. The PGA value of 0.2 *g* approximately corresponds to Modified Mercalli Intensity (MMI) of VII; thus '*considerable damage*' may occur at these locations according to the USGS (https://earthquake.usgs.gov/learn/topics/mercalli.php). When localized intense shaking occurs near high-density human settlements, a greater number of people will be affected simultaneously by the event, and thus the overall impact becomes severer. Notably, with the consideration of spatially correlated ground motion fields, opposite (fortunate) situations can happen, i.e. localized intense shaking occurs in remote, less-populated areas. The affected population maps for different PGA values are also useful for understanding the regional impact of major seismic events in terms of exposure.

Lastly, scenario maps of building collapse for the continuous and Bilila rupture cases are presented in Figure 6c and Figure 6f, respectively. In generating the building collapse maps, seismic fragility models of two building types are used for urban and rural areas (Figure 5b). In this study, the urban areas are identified as grid cells having more than 4000 people (per 0.02° by 0.02° cell). The proportions of '*poor*' and '*moderate*' houses in terms of seismic resistance, as in Figure 5b, are determined based on the existing literature (UN-Habitat 2010) and the survey results (Section 2.2.3), and are assigned as 25% and 75% in urban areas and 75% and 25% in rural areas. The generated building collapse maps show that the spatial distributions of building collapse cover larger areas than those of the affected population shown in Figure 6b and Figure 6e. This is because poorly constructed buildings could be destroyed by ground shaking less than 0.2 *g* (see Figure 5b), illustrating the severe deficiency of masonry buildings in Malawi. With the increase of earthquake magnitude, spatial areas that experience building collapse become larger. This highlights the scale effect of regional impact due to earthquake magnitude, and is of critical importance for risk managers who are responsible for

disaster risk mitigation and response-recovery actions.

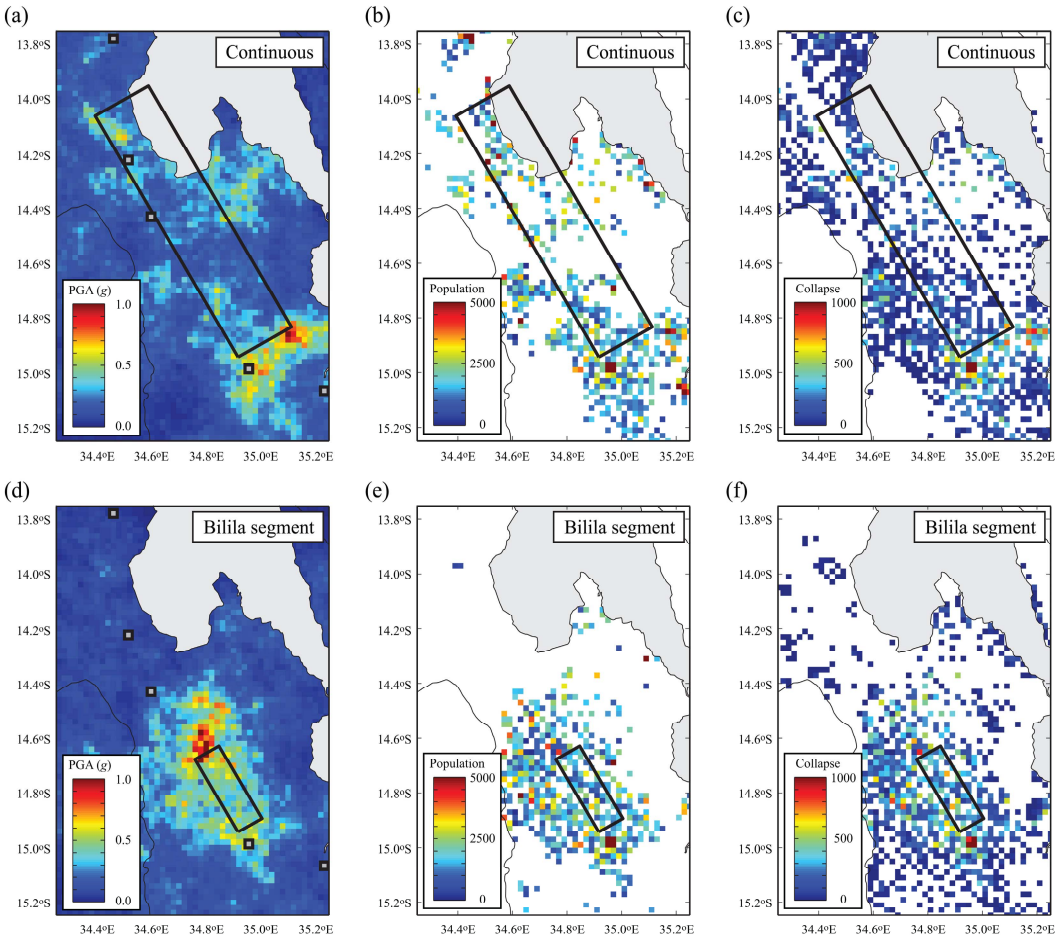

Figure 6. (a-c) Scenario PGA map, scenario affected population map experiencing PGA > 0.2 *g*, and building collapse map for the entire rupture of the Bilila-Mtakataka Fault, and (d-f) scenario PGA map, scenario affected population map experiencing PGA > 0.2 *g*, and building collapse map for the rupture of the Bilila segment

3.2 Regional Earthquake Impact on Population and Buildings

The major advantages of the probabilistic seismic hazard and risk maps that are shown in Figure 6, with respect to conventional deterministic shake maps are that a range of earthquake impact forecast can be produced. To demonstrate the usefulness of probabilistic earthquake impact assessments, the cumulative distribution functions (CDF) of people who experience PGA > 0.2 *g* are evaluated using 1,000 probabilistic shake maps for the seven rupture cases that are listed in Table 1. The results are shown in Figure 7a. For comparison, results for the deterministic cases are also included as symbols in the figure. Figure 7a indicates that the spread of the CDFs of the affected population is relatively large, and the deterministic estimates of the affected population correspond to different probability levels in terms of the CDF of the affected population. Importantly, the deterministic assessments of the affected population cannot capture the extreme situations (deterministic results mostly corresponding to 0.3- to 0.6-fractile of the probability distribution), and potentially leading to misinformed risk management decisions.

To further investigate the effects of the probabilistic approach in evaluating the building collapse risk, the CDFs of the number of building collapse are obtained based on 1,000 probabilistic shake maps for the seven rupture cases. The results are shown in Figure 7b. The general trends of the results are similar to those of Figure 7a. The figure indicates that for the worst-case rupture scenario of the entire BMF, the range between 0.1-fractile and 0.9-fractile differs from about 120,000 building collapses to

about 320,000 building collapses, while the median estimate is about 210,000 building collapses. Thus the differences of the building collapse numbers with respect to the deterministic seismic risk estimate can be as large as the factor of 2. Using these results, disaster risk managers can make informed risk management decisions more effectively, rather than relying on single scenario.

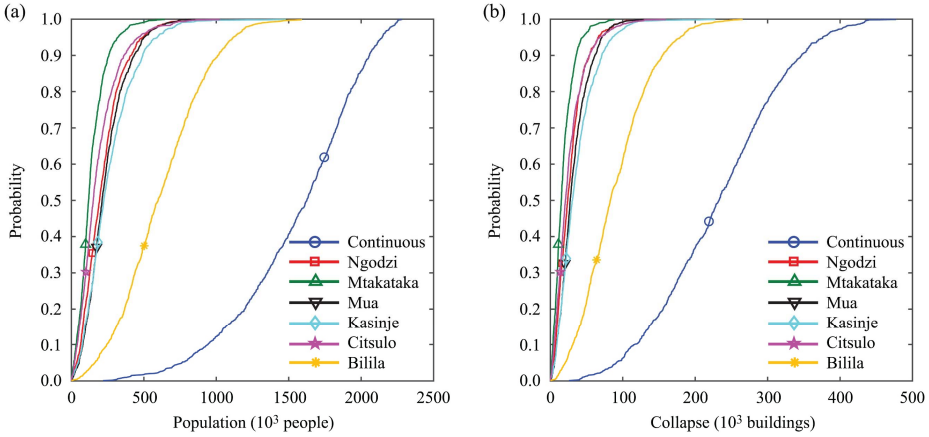

Figure 7. (a) Cumulative distribution functions of affected population experiencing PGA > 0.2 *g* for the seven rupture scenarios, and (b) cumulative distribution functions of building collapse for the seven rupture scenarios

4. CONCLUSIONS

This study developed a scenario-based earthquake impact assessment tool for Malawi using improved information on possible earthquake sources, local building characteristics, and seismic vulnerability functions. The application of the tool was demonstrated by focusing upon the Central-Southern Malawi region near the Bilila-Mtakataka Fault. The developed tool can generate multiple realizations of probabilistic shake maps, impacted exposure maps, and building collapse maps by incorporating the key uncertainties in ground motion simulations and seismic fragility evaluations. Moreover, the tool can generate the probability distributions of the important exposure and risk metrics for seismic risk management purposes. In the future, the tool can be further extended to carry out multi-scenario-based seismic hazard and risk assessments and can serve to implement performance-based earthquake engineering methods.

5. ACKNOWLEDGMENTS

This work is funded by the Engineering and Physical Sciences Research Council through the ***PREPARE*** project (Enhancing *PREP*aredness for *E*ast *A*frican Countries through Seismic *R*esilience *E*ngineering; EP/P028233/1).

6. REFERENCES

Biggs J, Nissen E, Craig T, Jackson J, Robinson DP (2010). Breaking up the hanging wall of a rift-border fault: the 2009 Karonga earthquakes, Malawi. *Geophysical Research Letters*, 37, L11305.

Boore DM, Stewart JP, Seyhan E, Atkinson GM (2014). NGA-West 2 equations for predicting PGA, PGV, and 5%-damped PSA for shallow crustal earthquakes. *Earthquake Spectra*, 30(3): 1057-1085.

Caliò I, Marletta M, Pantò B (2012). A new discrete element model for the evaluation of the seismic behaviour of unreinforced masonry buildings. *Engineering Structures*, 40: 327-338.

De Luca F, Vamvatsikos D, Iervolino I (2013). Near-optimal piecewise linear fits of static pushover capacity curves for equivalent SDOF analysis. *Earthquake Engineering & Structural Dynamics*, 42(4): 523-543.

Drucker DC, Prager W (1952). Soil mechanics and plastic analysis or limit design. Quarterly of Applied Mathematics, 10(2): 157-165.

Earle PS, Wald DJ, Jaiswal KS, Allen TI, Marano KD, Hotovec AJ, Hearne MG, Fee JM (2009). Prompt assessment of global earthquakes for response (PAGER): a system for rapidly determining the impact of global earthquakes worldwide. United States Geological Survey, USA.

Goda K, Hong HP (2008). Spatial correlation of peak ground motions and response spectra. *Bulletin of the Seismological Society of America*, 98(1): 354-365.

Goda K, Gibson ED, Smith HR, Biggs J, Hodge M (2016). Seismic risk assessment of urban and rural settlements around Lake Malawi. *Frontiers in Built Environment*, 2(30).

Gupta HK, Malomo S (1995). The Malawi earthquake of March 10, 1989: report of field survey. *Seismological Research Letters*, 66(1), 20-27.

Hodge M, Biggs J, Goda K, Aspinall WP (2015). Assessing infrequent large earthquakes using geomorphology and geodesy in the Malawi Rift. *Natural Hazards*, 76(3): 1781-1806.

Hodge M, Fagereng A, Biggs J, Mdala HS (2017). Fault-scale controls on rift geometry: the Bilila-Mtakataka Fault, Malawi. *AGU Fall Meeting*, New Orleans, USA, Abstract 231065.

Jackson J, Blenkinsop T (1993). The Malawi Earthquake of March 10, 1989: Deep faulting within the East African Rift System. Tectonics, 12(5): 1131-1139.

Jackson J, Blenkinsop T (1997). The Bilila-Mtakataka fault in Malawi: an active, 100-km long, normal fault segment in thick seismogenic crust. *Tectonics*, 16(1): 137-150.

Lagomarsino S, Penna A, Galasco A, Cattari S (2013). TREMURI program: an equivalent frame model for the nonlinear seismic analysis of masonry buildings. *Engineering Structures*, 56: 1787-1799.

National Statistical Office of Malawi (2008). 2008 Population and Housing Census. Available at: http://www.nsomalawi.mw/index.php?option=com_content&view=article&id=106&Itemid=6.

Ngoma I (2005). State-of-art and sustainable improvements of traditional Sub-Saharan African housing with special reference to Malawi, *Ph.D. Thesis*, University of Pisa, Italy.

McKenna F (2011). OpenSees: a framework for earthquake engineering simulation. *Computing in Science & Engineering*, 13(4): 58-66.

Milani G, Lourenço P, Tralli A (2007). 3D homogenized limit analysis of masonry buildings under horizontal loads. *Engineering Structures*, 29(11): 3134-3148.

Poggi V, Durrheim R, Tuluka GM, Weatherill G, Gee R, Pagani M, Nyblade A, Delvaux D (2017). Assessing seismic hazard of the East African Rift: a pilot study from GEM and AfricaArray. *Bulletin of Earthquake Engineering*, 15(11): 4499-4529.

Raka E, Spacone E, Sepe V, Camata G (2015). Advanced frame element for seismic analysis of masonry structures: model formulation and validation. *Earthquake Engineering & Structural Dynamics*, 44(14): 2489-2506.

Quagliarini E, Maracchini G, Clementi F (2017). Uses and limits of the Equivalent Frame Model on existing unreinforced masonry buildings for assessing their seismic risk: a review. *Journal of Building Engineering*, 10, 166-182.

Thingbaijam KKS, Mai PM, Goda K (2017). New empirical earthquake-source scaling laws. *Bulletin of the Seismological Society of America*, 107(5): 2225-2246

UN-Habitat (2010). Malawi: urban housing sector profile. Available at: https://unhabitat.org/books/malawi-urban-housing-sector-profile/.

Wald DJ, Worden BC, Quitoriano V, Pankow KL (2005). ShakeMap manual: technical manual, user's guide, and software guide. United States Geological Survey, USA.

Wald DJ, Allen TI (2007). Topographic slope as a proxy for seismic site conditions and amplification. *Bulletin of the Seismological Society of America*, 97(5): 1379-1395.

World Housing Encyclopedia (2002). World housing encyclopedia database for Malawi. Available at http://db.world-housing.net/list.